Normal Contact Stiffness of Elastic Solids with Fractal Rough Surfaces

Roman Pohrt and Valentin L. Popov
Berlin University of Technology, 10623 Berlin, Germany
(Received 24 August 2011; published 5 March 2012)

Using the boundary element method, we calculate the normal interfacial stiffness and constriction resistance of two elastic bodies with randomly rough surfaces and varying fractal dimensions. The contact stiffness as a function of the applied normal force can be approximated by a power law, with an exponent varying from 0.51 to 0.77 for fractal dimensions varying from 2 to 3.

DOI: 10.1103/PhysRevLett.108.104301 PACS numbers: 46.55.+d, 62.20.Qp, 73.40.Cg

The surface roughness has a large influence on many physical phenomena such as friction, wear, sealing, adhesion, and electrical as well as thermal contacts [1]. Bowden and Tabor [2] were the first to realize the importance of the roughness of the surfaces of bodies in contact. Because of this roughness, the real contact area between the two bodies is typically orders of magnitude smaller than the apparent contact area. The works of Bowden and Tabor triggered an entirely new line of theory for contact mechanics regarding rough surfaces in the 1950s and 1960s with basic contributions by Archard [3] and Greenwood and Williamson [4]. The main result of these examinations was that the contact area between rough elastic surfaces is approximately proportional to the normal force. In the past years, the contact properties of bodies with rough surfaces have been extensively studied [5–8], the main focus being put on the determination of the real contact area for self-affine surfaces with relevant fractal dimensions. It was found that the contact area A is proportional to the normal force F_N and inversely proportional to the rms slope of the surface ∇h: $A = \kappa F_N/(E^* \nabla h)$, where κ is near 2 and $E^* = [(1 - \nu_1^2)/E_1 + (1 - \nu_2^2)/E_2]^{-1}$ denotes the effective elastic modulus. E_1, E_2, ν_1, and ν_2 are the Young's moduli and Poisson's ratios, respectively, of the contacting bodies. Another important contact quantity, which is, however, much less investigated, is the contact length:

$$\tilde{L} = \frac{1}{E^*} \frac{\partial F_n}{\partial d}, \tag{1}$$

wherein d is the approach of two remote points within the contacting bodies. The contact length can be roughly defined as a sum of diameters of all contact regions (for details, see [1]). It determines many practically important properties, such as contact stiffness or electrical or thermal conductivity. The quantities related to the contact length are all connected with each other by exact analytical relations. For example, the contact conductance Λ is linearly proportional to the incremental stiffness: $k = \frac{\partial F_n}{\partial d} = E^*(\rho_1 + \rho_2)\Lambda/2$ [9], where ρ_1 and ρ_2 are the resistivities of the contacting bodies. Thus, investigation of either incremental stiffness or conductivity would suffice for determining this whole class of properties.

Numerical determination of the contact stiffness is more sophisticated than the calculation of the contact area, as the saturation stiffness value corresponding to an ideal contact is reached more quickly than an ideal "full material contact" [1]. Recently, the contact stiffness was studied numerically with the help of molecular dynamics [10] as well as with the boundary element method and analytically in the frame of Persson's contact theory [11]. According to the theory of Greenwood and Williamson [4], the contact stiffness k is approximately proportional to the normal force $k \approx \xi F_N/h$, where h is the rms roughness and ξ a constant of the order of unity. According to the theory of Persson, an exact proportionality [12] exists between the normal force and its derivative with respect to the mean surface separation. Numerical simulations carried out in Refs. [10,11] as well as experiments presented in Ref. [12] seem to support this conclusion. Note that we investigate in this Letter the total contact stiffness, while in Refs. [10,11] the interfacial contact stiffness was studied. Although a different definition of the contact stiffness is used in these works, the results should be the same for small normal forces, when the bulk deformation can be neglected. Unfortunately, results for small normal forces were not presented in Refs. [10,11]. Furthermore, in Ref. [10], simulations partially have been done with the help of molecular dynamics; thus, plastic deformation of surfaces cannot be excluded. In the present Letter, we consider only a pure elastic contact.

We calculated the normal stiffness of contact between bodies with self-affine fractal surfaces. As a test, we reproduced [13] the earlier results on the dependence of the real contact area on the normal force [7] and investigated the dependence of the contact stiffness on the normal force as it was done recently in Refs. [10,11]. In contrast to Ref. [10], however, we studied this dependence with the boundary element method for a finite squarish indenter over a wider range of normal forces. Lowering the normal forces resulted in an essential nonlinearity in the stiffness. Results for low to medium forces can be reproduced much

 © 2012 American Physical Society

better by a power-law dependence $k \propto F_N^{\alpha}$ with α ranging from 0.51 to 0.77, corresponding to a variation of fractal dimension from 2 to 3.

We considered the normal contact between an elastic solid having a randomly rough self-affine surface with a flat rigid body. The surface topography of the elastic body was characterized by its power spectrum $C_{2D}(q)$. For self-affine fractal surfaces, the spectral density has a power-law dependency on the wave vector

$$C_{2D}(q) = \text{const} \times \left(\frac{q}{q_0}\right)^{-2(H+1)}, \tag{2}$$

wherein H is the Hurst exponent, ranging from 0 to 1 [6]. It is directly related to the fractal dimension of a surface $D_f = 3 - H$. The surface topography is calculated in the two-dimensional case with the help of the power spectrum according to

$$h(\vec{x}) = \sum_{\vec{q}} B_{2D}(\vec{q}) \exp\{i[\vec{q} \cdot \vec{x} + \phi(\vec{q})]\} \tag{3}$$

with

$$B_{2D}(\vec{q}) = \frac{2\pi}{L}\sqrt{C_{2D}(\vec{q})} = \bar{B}_{2D}(-\vec{q}) \tag{4}$$

and the phases $\phi(\vec{q}) = -\phi(-\vec{q})$, which are randomly distributed on the interval $[0, 2\pi)$. Figure 1 shows a graphical representation of typical surface shapes for different values of D_f. Rough surfaces were generated on a square A_0 with an equidistant discretization of 2049×2049 points. We applied the boundary element method with an iterative multilevel algorithm to obtain the pressure distribution for a series of dimensionless normal forces. The incremental stiffness k was calculated by evaluating the differential quotient of force and indentation depth. All values were obtained by an ensemble averaging over 60 surface realizations having the same power spectrum. At complete contact, the stiffness is proportional to $E^*\sqrt{A_0}$. It approaches a saturated value of $k_{\text{sat}} = 1.1419E^*\sqrt{A_0}$, corresponding to the theoretical value for a squarish indenter. Thus, it is reasonable to define a dimensionless stiffness as $\bar{k}_i = k(d_i)/(E^*\sqrt{A_0})$. In Fig. 2, the stiffness can be regarded as saturated in the first 3 configurations.

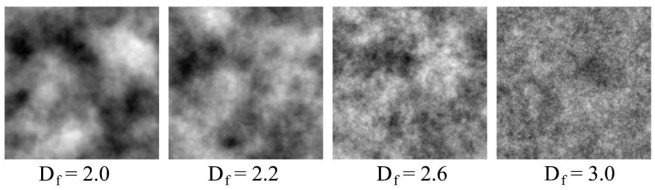

FIG. 1. Graphical representation of fractal surfaces having different fractal dimensions. Darker colors denote higher peaks in topography. Data have been scaled for optimal contrast in each picture.

The whole range of calculated dependencies of the contact stiffness on normal force for six fractal dimensions ($D_f = 2.0, 2.2, 2.4, 2.6, 2.8, 3.0$) is shown in Fig. 3. For small to medium forces, the logarithm of stiffness is very accurately proportional to the logarithm of the normal force. The stiffness is thus a power function of the normal force $\bar{k} = \text{const} \times \bar{F}_N^{\alpha}$. The power α can be fitted as

$$\alpha \approx 0.2567 D_f \tag{5}$$

(see also Fig. 4). This result qualitatively differs from the prediction $k \approx \xi F_N/h$ of the Greenwood-Williamson model but corresponds much better to the results obtained in the frame of method of reduction of dimensionality [14,15] and reported in Ref. [16] (Chapter 9, p. 93) as well as to experimental measurements of the contact stiffness reported in Ref. [17].

Based on the power law, we searched for an analytical approximation for the contact stiffness. Under the assumption that the only parameters appearing in the stiffness-force dependence are the elastic modulus E^* as well the rms roughness h and that it is a power-law function of all arguments, the problem contains only the following independent dimensionless variables: dimensionless stiffness $k/(E^*\sqrt{A_0})$, dimensionless force $F/(E^*A_0)$, and

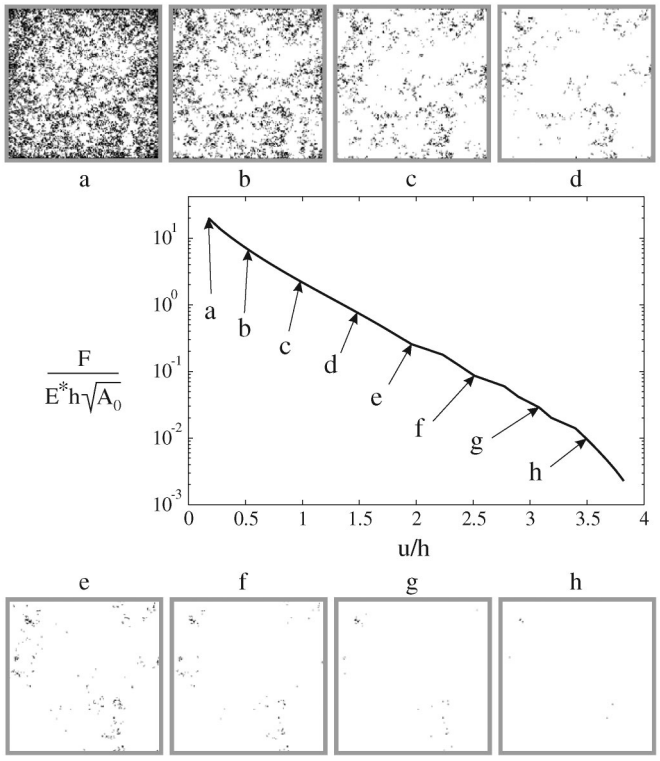

FIG. 2. Dependency of the dimensionless normal force on the mean surface separation u for $D_f = 2.8$. Subplots show the real contact area for a specific surface realization. Even though only a fraction of the surface is in intimate contact in plots (a)–(c), the saturated value of the normal stiffness is already reached. (See Fig. 3 at corresponding normal force.)

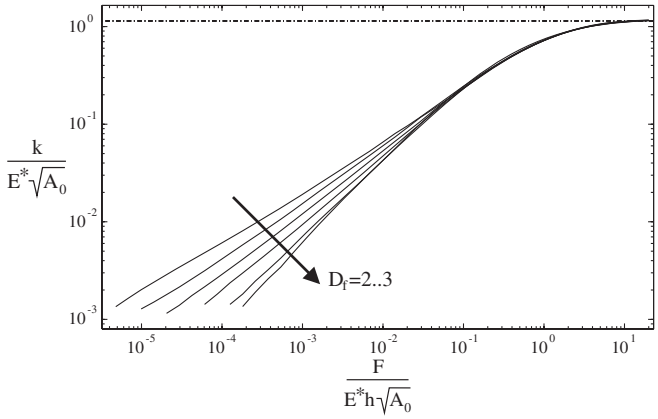

FIG. 3. Dependencies of the dimensionless normal stiffness on the dimensionless normal force. Curves are shown for $D_f = \{2.0; 2.2; 2.4; 2.6; 2.8; 3.0\}$. The dashed line represents the theoretical value for the saturated stiffness of a squarish indenter $\tilde{k}_{\mathrm{sat}} = 1.1419$. Below the saturation, a power-law dependence is observed.

dimensionless rms roughness $h/\sqrt{A_0}$. The general form of a power function connecting these variables is $k/(E^*\sqrt{A_0}) = \zeta(\frac{F}{E^* A_0})^{\alpha}(\frac{h^2}{A_0})^{\delta}$, where ζ is a dimensionless constant. This dependence must possess the following strict scaling properties. If the vertical scale of the surface inhomogeneity is multiplied by a certain factor, then the contact configuration does not change, provided that the force F and the indentation depth u_z are both multiplied by this factor. This means that k does not change and the relation $\alpha + 2\delta = 0$ is valid; it follows that $\delta = -\alpha/2$. In addition, at a given contact configuration, both the force and the stiffness must be strictly proportional to the effective elastic modulus E^*, which is already fulfilled by the above equation. The only possible general power dependence of the contact stiffness on force obeying these scaling relations is

$$\frac{k}{E^*\sqrt{A_0}} = \zeta\left(\frac{F}{E^* h\sqrt{A_0}}\right)^{\alpha}. \tag{6}$$

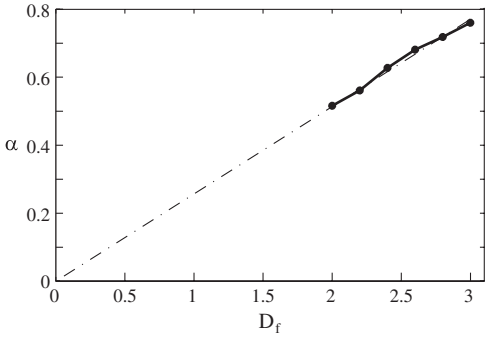

FIG. 4. Dependence of power α in Eq. (6) on the fractal dimension of a surface. The dashed line corresponds to the chosen approximation $\alpha \approx 0.2567 D_f$.

The dependence of the coefficient ζ on the fractal dimension can be approximated by $\zeta = \pi D_f/10$. Thus, we finally find the following approximation for the stiffness:

$$\frac{k}{E^*\sqrt{A_0}} = \frac{\pi D_f}{10}\left(\frac{F}{E^* h\sqrt{A_0}}\right)^{0.2567 D_f}. \tag{7}$$

To prove this relation, the value of $\tilde{F} = \{[10/(\pi D_f)] \times [k/(E^*\sqrt{A_0})]\}^{1/(0.2567 D_f)}$ is plotted against the dimensionless normal force $F/(E^* h\sqrt{A_0})$ in Fig. 5. The data for all forces and all fractal dimensions collapse to one master curve. Of course, these results are valid only for pure elastic bodies. In real contacts, on increasing the load over wider range of values, one can expect plastic deformations to come into play.

Using the exact relation between the constriction conductance Λ and the incremental stiffness of a contact of two bodies [9], we can straightforwardly write down an expression for the contact conductance of bodies having rough surfaces and resistivities ρ_1 and ρ_2:

$$\Lambda = \frac{\pi D_f\sqrt{A_0}}{5(\rho_1 + \rho_2)}\left(\frac{F}{E^* h\sqrt{A_0}}\right)^{0.2567 D_f}. \tag{8}$$

In conclusion, the boundary element method was used to study the normal stiffness of elastic bodies with self-affine randomly rough surfaces with fractal dimensions ranging from 2 to 3. As a test, we reproduced the linear dependence of the contact area on the normal force predicted by Persson's theory but obtained a nonlinear behavior of the incremental normal stiffness. This happens to be a

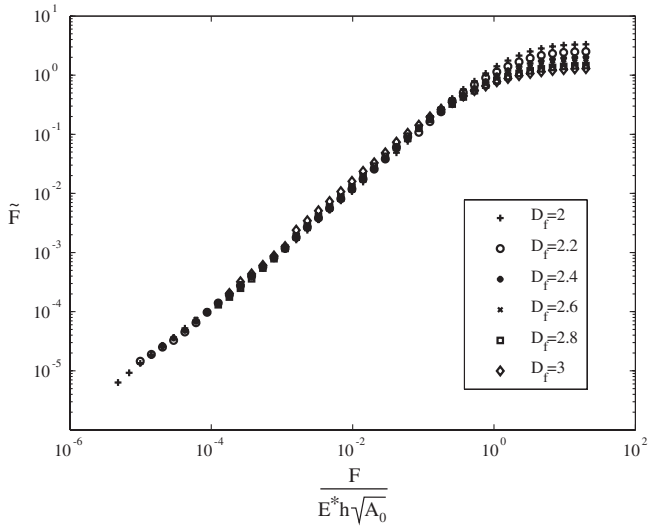

FIG. 5. A plot of $\tilde{F} = \{[10/(\pi D_f)][k/(E^*\sqrt{A_0})]\}^{1/(0.2567 D_f)}$ shows that the valid range for Eq. (7) comprises 4 orders of magnitude in dimensionless F with the chosen resolution of 2049×2049. Numerical limitations prevented us from investigating smaller normal forces, but we believe the power law to correctly describe the asymptotical behavior as well [13]. For very high normal forces, Eq. (7) no longer holds due to the saturation of the normal stiffness.

power-law dependence of the normal force with the power ranging from 0.51 for a fractal dimension of $D_f = 2$ to 0.77 for a fractal dimension of $D_f = 3$. Furthermore, it has powerlike dependencies on rms roughness, elastic modulus, and the nominal area of contact. We have found simple analytical approximations for contact stiffness and contact conductance, which are valid over more than 4 orders of magnitude of normal force.

Discussions with A. Filippov are gratefully acknowledged. The authors are also grateful to R. Wetter for attracting attention to the paper by Barber. This material is based upon work supported by AiF (Grant No. KF2293701WZ9).

[1] V. L. Popov, *Contact Mechanics and Friction* (Springer, New York, 2010).
[2] F. P. Bowden and D. Tabor, *The Friction and Lubrication of Solids* (Clarendon, Oxford, 1986).
[3] J. F. Archard, Proc. R. Soc. A **243**, 190 (1957).
[4] J. A. Greenwood and J. B. P. Williamson, Proc. R. Soc. A **295**, 300 (1966).
[5] S. Hyun, L. Pei, J.-F. Molinari, and M. O. Robbins, Phys. Rev. E **70**, 026117 (2004).
[6] B. N. J. Person, Surf. Sci. Rep. **61**, 201 (2006).
[7] S. Hyun and M. O. Robbins, Tribol. Int. **40**, 1413 (2007).
[8] C. Campana and M. H. Müser, Phys. Rev. B **74**, 075420 (2006).
[9] J. R. Barber, Proc. R. Soc. A **459**, 53 (2003).
[10] S. Akarapu, T. Sharp, and M. O. Robbins, Phys. Rev. Lett. **106**, 204301 (2011).
[11] C. Campana, B. N. J. Persson and M. H. Müser, J. Phys. Condens. Matter **23**, 085001 (2011).
[12] B. Lorenz and B. N. J. Persson, J. Phys. Condens. Matter **21**, 015003 (2009).
[13] See Supplemental Material at http://link.aps.org/supplemental/10.1103/PhysRevLett.108.104301 for results for the contact area taken from the simulation and dependence on grid size.
[14] T. Geike and V. L. Popov, Phys. Rev. E **76**, 036710 (2007).
[15] T. Geike and V. L. Popov, Tribol. Int. **40**, 924 (2007).
[16] V. L. Popov, *Kontaktmechanik und Reibung* (Springer, Berlin, 2009).
[17] R. Buzio *et al.*, Nature Mater. **2**, 233 (2003).